Population genomic time series data of a natural population suggests adaptive tracking of environmental changes

Markus Pfenninger[1,2,3] & Quentin Foucault[1,2]

[1]Dept. Molecular Ecology, Senckenberg Biodiversity and Climate Research Centre, Senckenberganlage 25, 60325 Frankfurt am Main, Germany

[2]Institute for Molecular and Organismic Evolution, Johannes Gutenberg University, Johann-Joachim-Becher-Weg 7, 55128 Mainz, Germany

[3] LOEWE Centre for Translational Biodiversity Genomics, Senckenberg Biodiversity and Climate Research Centre, Senckenberganlage 25, 60325 Frankfurt am Main, Germany

Running head: adaptive tracking in natural population

Corresponding author: Markus Pfenninger

Markus.Pfenninger@senckenberg.de

Abstract

Natural populations are constantly exposed to fluctuating environmental changes that negatively affect their fitness in unpredictable ways. While theoretical models show the possibility of counteracting these environmental changes through rapid evolutionary adaptations, there have been few empirical studies demonstrating such adaptive tracking in natural populations.

Here, we analysed environmental data, fitness-related phenotyping and genomic time-series data sampled over three years from a natural *Chironomus riparius* (Diptera, Insecta) population to address this question. We show that the population's environment varied significantly on the time scale of the sampling in many selectively relevant dimensions, independently of each other. Similarly, phenotypic fitness components evolved significantly on the same temporal scale (mean 0.32 Haldanes), likewise independent from each other. The allele frequencies of 367,446 SNPs across the genome showed evidence of positive selection. Using temporal correlation of spatially coherent allele frequency changes revealed 35,574 haplotypes with more than one selected SNP. The mean selection coefficient for these haplotypes was 0.30 (s.d. = 0.68). The frequency changes of these haplotypes clustered in 46 different temporal patterns, indicating concerted, independent evolution of many polygenic traits. Nine of these patterns were strongly correlated with measured environmental variables.

Thus, our results suggest that the natural population of *C. riparius* tracks environmental change through rapid polygenic adaptation in many independent dimensions. This is further evidence that natural selection is pervasive at the genomic level and that evolutionary and ecological time scales may not differ at all, at least in some organisms.

Introduction

Most natural environments consist of an almost infinite number of aspects and parameters that are constantly changing in space and time (Kingsolver *et al.*, 2012). Organisms in such habitats therefore potentially have to deal with a fluctuating selective regime (Bell, 2010) where the direction of selection frequently changes (Siepielski *et al.*, 2009). The question is whether and to what extent natural populations rapidly and constantly adapt to the fluctuations in their environment in a process termed adaptive tracking (Vander Wal *et al.*, 2013). The answer is crucial for our understanding of the relative roles of adaptation vs. phenotypic plasticity (King & Hadfield, 2019), eco-evolutionary processes (Rudman *et al.*, 2018), the maintenance of genetic variation (Barton & Keightley, 2002) and the process of balancing selection in natural populations (Abdul-Rahman *et al.*, 2021).

Theoretical work has shown that rapid adaptation, a prerequisite for adaptive tracking, is possible almost in real time in natural populations (Messer & Petrov, 2013; Botero *et al.*, 2015; Matuszewski *et al.*, 2015), in particular if polygenic traits are the target of selection (Jain & Stephan, 2017; Barghi *et al.*, 2020). However, despite the importance of the question whether and to what extent selective tracking plays a role in nature, empirical studies are rare. There are a few examples of selective tracking of the fluctuating environment for phenotypic traits (Grant & Grant, 1989; Marrot *et al.*, 2017; de Villemereuil *et al.*, 2020). In particular the selectively driven beak variability of Galapagos finches in response to different weather conditions in different years, is the classic example of very rapid evolutionary adaptation to a variable environment (Boag & Grant, 1981). On the molecular level, there are several demonstrations of rapid selectively driven changes (Yang *et al.*, 2016; Margres *et al.*, 2017; Bitter *et al.*, 2019; Zong *et al.*, 2021). Seasonally selected polymorphisms with correlated allele frequency trajectories were also observed in natural populations of a dipteran species, *Drosophila melanogaster* (Bergland *et al.*, 2014; Croze *et al.*, 2017). However, studies bringing together the observed temporal fitness differences among different phenotypes with the underlying molecular variants are scarce. In a complex semi-natural experiment (Rudman *et al.*,

2021), could demonstrate adaptive tracking on both the phenotypic and genomic level. However, it has been stressed that real-world examples from natural populations are needed (Hendry, 2019).

In a recent article Pfenninger et al. (2022) could show with population genomic time series data and experiments that a natural population of the non-biting midge *Chironomus riparius* (Meigen, 1803) selectively tracked a short-term weather event. Moreover, long term genomic time series data suggested that the spatially unlinked alleles involved in the investigated polygenic trait under selection changed temporally in a correlated fashion over a longer period (Pfenninger *et al.*, 2022). This raised the question whether there are more spatially unlinked haplotypes in the genome that change over time in correlated fashion, thus indicating independent responses to the respectively same selective forces. Or, in other words, does this species generally adaptively track the environmental changes in its habitat? To demonstrate adaptive tracking, it is necessary to show that fitness-related phenotypic and selection driven genomic changes happen on the same time scale as selectively relevant environmental changes.

Here, we used environmental data, fitness related phenotyping and population genomic time series data of the same natural *C. riparius* population to tackle this question. *Chironomus riparius* is a multivoltine species with up to 15 generations per year in Europe (Oppold *et al.*, 2016). Therefore, the different generations are subjected to widely varying environmental conditions. Accordingly, extensive research on temperature and photoperiod has shown that several traits can and do adapt locally (Waldvogel *et al.*, 2018), and temporally among seasons (Foucault *et al.*, 2018; Doria *et al.*, 2022a). But also other factors are known to act as selection pressures on this species (e.g. organic load, Kraak *et al.* (2000), conductivity, (Pfenninger & Nowak 2008), nitrogen, (Nemec *et al.* 2012), temperature, (Nemec *et al.* 2013) and anthropogenic substances, (Nowak *et al.* 2009). The high effective and demographic population size (> 1,000,000, Waldvogel *et al.* (2018)) and the very high number of offspring per breeding pair (400-800) allows for rapid adaptation (Pfenninger & Foucault, 2020). A range of genomic resources and parameters are available (Schmidt *et al.* 2020; Oppold & Pfenninger 2017) and established routines for evolutionary experiments in the laboratory exist

90 (Foucault *et al.*, 2019b), which makes the species a suitable object to test the hypothesis that
91 adaptive tracking takes place in natural populations. Here, we addressed the following questions:

92 - Did known selection pressures change over the periods monitored in the natural population,
93 thus providing a fluctuating selective regime?
94 - Is there fitness-related phenotypic evolution on the same time scale in the population?
95 - Can we find evidence for selection-driven allele frequency changes in the genome?
96 - Are there spatially unlinked selected haplotypes whose allele frequencies evolve in a
97 temporally correlated fashion, indicative of polygenic adaptation?
98 - If so, how many of such selected trajectory clusters can we identify?
99 - Are the frequency changes of the haplotypes in these clusters correlated with recorded
100 environmental changes?

101 Material and Methods

102 *Sampling*

103 In February 2016, more than 500 living red *thummi*-type chironomid larvae were sampled with a
104 sieve at a single site situated in a small river (Hasselbach, Hessen, Germany 50.167562°N,
105 9.083542°E) following the protocol of (Foucault *et al.*, 2019b). The specimen's specific identity was
106 ascertained by DNA-barcoding of a mitochondrial (COI) and a nuclear locus (L44). Eighty thus
107 identified *C. riparius* were pooled and subjected to PoolSeq sequencing (see below). The sampling
108 was likewise repeated in September 2016, assuming that the two annual samples thus were
109 subjected to the selective extremes of the winter and summer season, respectively. This sampling
110 scheme was repeated for the two following years, 2017 and 2018, resulting in a time series of six
111 population pools (NP0-NP5). From February to September, the population produced about seven
112 generations, in the period from autumn to early spring about three. The entire sampling period thus
113 covered about 27 generations (Suppl. Fig. 1). We used additional *C. riparius* individuals from the field,
114 sampled at the same time as the individuals for genomic analysis except for September 2018, to
115 perform standardised life cycle fitness tests at three temperatures (14°C, 20°C and 26°C).

Environmental parameters

Mean monthly water parameters for the period 2009-2018 were obtained from the Hasselbach water treatment plant of the Abwasserverband Freigericht. The values were continuously measured automatically in the river past the outflow, less than 50 m from the sampling site. The following parameters were recorded: water temperature [°C], conductivity [mS/cm], oxygen, biological oxygen demand (BOD), chemical oxygen demand (COD), NH_4, NO_3, NO_2, N_{tot} and PO_4, all [mg/l]. To assess the similarity of the entirety of the parameters over time, the monthly means were summarised in a seasonal mean for the period before sampling, *i.e.* from March to September and from October to February. These values were subjected to a Principal Components Analysis (PCA). Temporal autocorrelation was calculated in Past 4 (Hammer *et al.*, 2001).

Phenotypic evolution

We used an established life cycle fitness test to assess three fitness component phenotypes of the natural population under standard conditions in a common garden experiment. The experiment was carried out at 14°C which corresponds to the annual average water temperature at the sampling site. A fraction of the sampled larvae from each sampling date was divided into five replicates (30 individuals each) and brought to hatch and reproduce. To distinguish phenotypic evolution from phenotypic plasticity, the resulting F1 generation was monitored for the parameters developmental rate (measured as emergence mean time 50 EmT50), fecundity (viable eggs per female), mortality (proportion of emerging midges) and a resulting overall fitness parameter (population growth rate per day). The assessed phenotypes are known to have a complex genetic basis (Doria *et al.*, 2022a). We tested with an ANOVA for significant changes in mean trait values. A detailed description of the life cycle fitness test can be found in (Foucault *et al.*, 2019b).

We calculated rates of phenotypic evolution among sampling dates for each trait in Haldanes (h) as:

$$h = \frac{\frac{(x_1 - x_2)}{s_p}}{g}$$

140 where x_n represent the mean trait value at the time point n, s_p the pooled standard deviation and g
141 the number of generations between the two time points (Haldane, 1949)

142 *Population genomic analyses of pooled samples*

143 DNA was extracted for each pool from the field or the experiment using the Qiagen blood and tissue
144 extraction kit on pooled samples of 80 larval head capsules, respectively. Integrity and quality of
145 extracted DNA was controlled using electrophoresis, and the DNA concentration for each samples
146 measured with a Qubit fluorimeter (Invitrogen).

147 Whole genome pool-sequencing was carried out on an Illumina MySeq with 250bp paired end reads.
148 Reads were trimmed using the wrapper tool autotrim (Waldvogel *et al.*, 2018) that integrates
149 trimmomatic (Bolger *et al.*, 2014) for trimming and fastQC (Andrews 2010) for quality control. The
150 trimmed reads were then mapped on the latest *C. riparius* reference genome (Schmidt *et al.*, 2020)
151 using the BWA mem algorithm (Li & Durbin, 2009). Low quality reads were subsequently filtered and
152 SNPs were initially called using samtools(Li *et al.*, 2009). The pipelines Popoolation and Popoolation2
153 (Kofler *et al.*, 2011a, 2011b) were used to call SNPs, remove indels, and to estimate genetic diversity
154 as Watterson's theta each pool. Allele frequencies for all SNPs with coverage between 15x and 70x
155 were estimated with the R library PoolSeq (Taus *et al.*, 2017).

156 *Identification of allele frequency trajectories with signs of selection*

157 Selected SNP loci were identified by allele-frequency changes (AFC) larger than expected by neutral
158 drift. First, Fisher's exact tests for the AFCs among all consecutive time points (NP0 > NP1 etc.) and
159 among the first and last sampling were calculated. This test identifies AFC larger than expected by
160 chance, but does not account for genetic drift expected. Therefore, neutral simulations were used to
161 compute false discovery rate q-values < 0.001 with parameters (number of SNPs, starting allele
162 frequencies in the ancestral population, sequence coverage, number of generations) matching those
163 of the respective sample. As effective population size, we used 15,000, which constitutes a very
164 conservative estimate (see (Waldvogel *et al.*, 2018)). All calculations and simulations were performed

165 with the R-library poolSeq (Taus *et al.*, 2017). A SNP locus was considered showing signs of selection
166 if at least one sampling interval or between the first and the last sample period had an AFC
167 significantly larger than expected. The allele frequency trajectory, i.e. the vector of allele frequencies
168 of such putatively selected SNP site over time was recorded.

169 *Inference of genome wide level of Linkage Disequilibrium*

170 The expected length of segregating haplotypes depends on the recombination rate and their age. The
171 former can be approximated by an estimate of linkage disequilibrium (LD,(Feder *et al.*, 2012). We
172 estimated the extent of LD and its decay using the maximum likelihood method of (Feder *et al.*,
173 2012) on one of the pools (NP0). This method exploits the haplotype information contained in
174 (paired) reads and has been shown to yield accurate estimates if mean LD decay to background levels
175 is shorter than the read length (Feder *et al.*, 2012).

176 *Clustering of spatially coherent SNPs into haplotypes*

177 Most SNPs showing larger than expected AFC are hitchhiking with the actually selected site in
178 selected haplotypes. The extent of such haplotypes was determined following the rationale of
179 (Franssen *et al.*, 2016) that physically linked variants following the same evolutionary trajectory
180 should show correlated allele frequencies through time. However, contrary to an experimental
181 evolution situation with a constant selection pressure, it could not be expected that the observed
182 AFC were always in the same direction. Since this is a prerequisite for the software used in Franssen
183 *et al.* (2016), we had to develop our own algorithm. Our algorithm considered consecutively all
184 temporal trajectories of significant SNPs along a scaffold. A SNP was added to a haplotype if the
185 absolute correlation coefficient of its temporal trajectory to any other trajectory of the SNPs already
186 in the haplotype equalled or exceeded a given threshold (0.75). This was repeated until the next SNP
187 position did not meet the criterion. The number of SNPs in the haplotype, its start and end position
188 and the mean allele frequency were then recorded and a new haplotype was started at the next
189 position considered. The analysis was carried out with a custom Python script.

190 *Validation of haplotypes*

191 Inferred haplotypes were validated with 30 whole genome resequenced individuals (25X coverage,
192 150 bp paired end reads) from all sampling periods. The reads from these individuals were quality
193 checked, mapped against the reference genome as described above and the genotypes called with
194 the GATK pipeline (Van der Auwera *et al.*, 2013). Consensus sequences of one hundred randomly
195 chosen haplotypes with more than 2 SNPs, including one neighbouring haplotype were extracted
196 from the individual VCF-files, aligned and phased with FastPhase in DNAsp (Rozas *et al.*, 2017). The
197 resulting phased alignments were checked for linkage of the previously identified target haplotype's
198 typical alleles and linkage equilibrium to the neighbouring haplotypes in the same software.

199 *Calculation of selection coefficients for haplotypes*

200 The selection coefficient *s* was calculated from the change in mean allele frequencies between
201 samplings for all selected haplotypes by the formula given in (Kimura, 1970). Assuming codominance
202 (i.e. h = 0.5), the selection coefficient *s* can be calculated as

203 $$s = 2 * (\ln\left(\frac{p_t}{1-p_t}\right) - \ln\left(\frac{p_0}{1-p_0}\right)) * t^{-1}$$

204 where p_0 is the allele frequency of the rising allele in the ancestral population and p_t its frequency in
205 generation t.

206 *Hierarchical clustering of mean haplotype trajectories*

207 For each haplotype, we calculated the mean allele frequency trajectory (MHT) over the allele
208 frequencies of all constituting SNPs. The matrix of absolute pairwise correlation coefficients among
209 all MHT was transformed into a distance matrix (1 – correlation coefficient), hierarchically clustered
210 with UPGMA and the resulting dendrogram plotted. The number of clusters considered was
211 determined by applying a clustering threshold of 0.25, corresponding to a minimum similarity of 0.75
212 of all MHT within a cluster.

213 To determine this threshold sensibly balancing between arbitrary lumping of actually different
214 trajectories and over-splitting of trajectories differing rather by stochastic fluctuations, we applied a
215 randomisation approach. From the empirical AFC distribution of all SNPs in the analysed set (i.e. at
216 least one significant AFC among consecutive sampling periods or between the first and last sampling
217 period, see above), we randomly drew, 1,000 times the empirically found number of MHTs. Starting
218 with a distance threshold of 0.05, we iteratively increased the threshold by 0.05. In each iteration,
219 the trajectories of the 1000 random MHTs were hierarchically clustered as described above and the
220 number of resulting clusters recorded. The simulated distribution was then compared to the
221 empirically observed number of clusters, applying the same threshold. The smallest distance
222 threshold for which the observed number of clusters was smaller than the 0.05 quantile of the
223 randomly simulated distribution was deemed appropriate for the analysis. This was the case for a
224 distance threshold of 0.25; i.e. the trajectories within a cluster showed a correlation of at least 0.75.
225 The analysis was performed with a custom Python script.

226 *Correlation of environmental parameters with haplotype trajectories*

227 The seasonal mean environmental parameters (see above) before the first and the respective period
228 between two sampling times were correlated to the means of all identified MHT patterns. To avoid
229 problems with multiple testing and lacking statistical power (Sjölander & Vansteelandt, 2019), we
230 employed a Bayesian implementation of a test on correlation with default values (Bååth, 2014). We
231 report only correlations with convincing posterior evidence (>95% posterior credibility) for positive,
232 respectively negative associations.

233 *GO-term enrichment analysis*

234 The annotated gene overlapping with a haplotype was identified as putative selection target. The
235 resulting gene lists for all member haplotypes of each MHT pattern were tested for over-
236 representation of GO terms in the category “biological function” in the R-library TopGO with a
237 Fisher’s exact test (Alexa & Rahnenführer, 2016).

238 ## Results

239 *Fluctuating enviroment*

240 Measured physico-chemical water parameters varied substantially through time (Figure 1, Suppl.
241 Fig.2). Comparison with a broken stick model suggested that the first two Principal Component axes
242 were meaningful. Axis 1 (51.8% of variation) of the PCA was mainly determined by parameters
243 describing organic water pollution (chemical oxygen demand, NH_4, biological oxygen demand,
244 conductivity), axis 2 (21.7%) reflected mostly seasonal changes (temperature, oxygen, PO_4, Figure 1).
245 The measured environmental regime never returned close to any previous state. This was mirrored
246 in the poor temporal autocorrelation of the parameters, except for the regular seasonal temperature
247 changes (Suppl. Fig. 3).

248 *Strong phenotypic evolution*

249 Exposed to the same standard conditions in a common garden setting, the F1 generation derived
250 from the natural population at different points in time showed signs of strong and rapid phenotypic
251 evolution, with idiosyncratic patterns across traits. The EmT50 value varied strongly and significantly
252 with the seasons ($F = 11,53$, d.f. = 4, $p = 5 \times 10^{-5}$) between 35.9 and 42.5 days, with an overlaid overall
253 decreasing trend (Figure 2A). Mean evolutionary rate for the trait between sampling dates was 0.29
254 Haldanes (min = 0.07, max = 0.42) with a reversal of direction between each sampling date (Figure
255 2A). Mortality varied also significantly, albeit marginally among sampling dates ($F = 3.25$, d.f. = 4, $p =$
256 0.03). Between 11% and 45% of the midges did not hatch in the laboratory environment (Figure 2B).
257 The rate of evolution was 0.22 (min = 0.07, max = 0.31) with two changes of direction (Figure 1B).
258 The strongest phenotypic evolution was observed for fecundity (Figure 2C). The mean fecundity
259 varied significantly between 84 and 286 offspring per female ($F = 6.07$, d.f. = 4, $p = 0.002$). The
260 evolutionary rate of change for the trait was on average 0.45 (min = 0.20, max = 0.96) standard
261 deviations per generation. The direction of the evolution changed twice during the period of
262 observation (Figure 2C). The resulting population fitness remained always positive (range = 1.112 –
263 1.145), but varied significantly among sampling dates ($F = 3.84$, d.f. = 4, $p = 0.02$, Figure 1D).

264 *Large parts of the genome showed evidence of selective evolution*

265 The genome-wide mean estimate of distance-dependent linkage disequilibrium (LD) dropped to a
266 mean r^2 of 0.5 within 10 base pairs and to the genome-wide background level of about 0.2 within 120
267 bp (Suppl. Fig. 5). Consequently, the expected haplotype structure was extremely short.

268 Allele frequency estimates for all sampling dates were obtained for 22,693,348 SNP positions in the
269 genome. Neutral drift simulations, taking observed sampling variance of the poolSeq approach into
270 account, showed that the chosen selection detection threshold of 2.0 $-\log_{10}p$ for an allele frequency
271 change (AFC) between consecutive sampling times or between the first and the last sampling implied
272 a false discovery rate of $q < 0.001$. This corresponded to an AFC of at least 0.15. Under the condition
273 of at least one selected AFC between any two consecutive sampling times or the first and the last
274 sampling time, identified a set of 367,446 SNPs with signs of selection.

275 Clustering spatially coherent SNPs with signs of selection into haplotypes resulted in 281,153
276 haplotypes of which 35,574 consisted of more than a single SNP. Of the 100 haplotypes randomly
277 chosen for validation, 98 showed the expected linkage between the marker SNPs of the haplotype
278 (Suppl. Fig. 6). In two cases, both with more than 2 haplotype marker SNPs, one of the marginal SNPs
279 was only slightly linked ($r < 0.6$). All haplotypes checked were distinct from their respective spatial
280 neighbours. Only the 35,574 haplotypes with more than a single SNP were retained for subsequent
281 analyses. In these, the average number of SNPs per haplotype was 3.30 +/- 2.64 (mean +/- s.d.). The
282 mean length of inferred haplotypes was 893.1 +/- 1790.3 bp. Neighbouring haplotypes on the same
283 scaffold were on average 3466.0 +/- 4293.5 bp apart. Of all 13,490 annotated genes in the genome,
284 5793 (= 42.9%) harboured at least one selected haplotype, some more.

285 The mean selection coefficient over all retained haplotypes was 0.30 with a standard deviation of
286 0.68. The latter is equivalent to the intensity of selection over time, and its much larger value relative
287 to the mean indicated large changes in magnitude and frequent reversals in the direction of selection
288 (Bell 2010).

289 *Clustering of haplotype trajectories*

290 To avoid using an arbitrary clustering threshold, we used a Monte-Carlo simulation approach.
291 Clustering of simulated random MHTs, drawn from the observed AFC distribution, indicated that a
292 clustering threshold of 0.75 yielded informative clusters without undue lumping (Suppl. Fig. 7).
293 Applying this threshold, the 35,574 MHTs were grouped into 46 distinct cluster (Fig. 2). The number
294 of MHT cluster members was highly different. The largest cluster (MHT16) contained 17,914
295 haplotype trajectories, the smallest merely three (MHT28), the mean was 816.8 (Suppl. Table 2).

296 *Correlation of haplotype trajectories to environmental parameter changes and GO analysis*

297 Nine MHT cluster patterns were highly correlated to measured water parameters in the period
298 before sampling. Three MHTs were correlated to changes in NO_3. One MHTs followed variation on
299 Biological Oxygen Demand (BOD) closely. Two other MHTs were associated to NO_2, MHT3 was
300 correlated to PO_4, MHT 38 to temperature, while the strongest association was found for MHT 34
301 and oxygen (Figure 3). For 44 of the 46 MHT clusters, at least one significantly enriched GO term was
302 found (Suppl. Table 2). Most enriched terms for the individual MHT clusters were on a very high
303 hierarchical level. Consequently, they were rather uninformative or affected only a small minority of
304 the genes with overlap to a selected haplotype. However, some hinted at a specific biological process
305 or supported the observed association of the MHT cluster to a measured physico-chemical variable.

306 The enriched terms for MHT4 (GO terms *0051704 multiorganism process*, *0006952 defense response*)
307 suggested reaction to a biological interaction. The largest cluster MHT16 contained hundreds of
308 genes involved in osmoregulation, reflected in the enrichment for GO terms *0055085*
309 *transmembrane transport* and *0006811 ion transport*. Despite affecting only about 20 genes, MHT36
310 showed an enrichment of terms associated with *porphyrin-containing compound biosynthetic process*
311 *(0006779)* and *pigment biosynthetic process (046148)*. Genes affected by MHT40 haplotypes were
312 enriched for signal transduction processes (*0007186 G protein-coupled receptor signaling pathway*),
313 perhaps in conjunction with hormones (*1901362 organic cyclic compound biosynthetic process*,

314 *0008202 steroid metabolic process*). MHT3 was enriched for term (*0006811 ion transport*). MHT39,
315 with *calcium (transmembrane) transport* (terms *0006813* and *0071805*), which is co-annotated to
316 *nitric-oxide synthase inhibitor activity*. There was an enrichment of the term *0005975 carbohydrate*
317 *metabolic process* in MHT21. MHT22 was enriched *for 0007688 sensory perception of smell* and
318 *0006979 response to oxidative stress*.

319 Discussion

320 *Complex and unpredictable multidimensional fluctuating selective regime*

321 The largely uncorrelated temporal changes as well as the observed range of the measured physico-
322 chemical water parameters suggested that the local environment presented a highly fluctuating,
323 multidimensional selective regime for *C. riparius*. For most of these parameters, the fitness relevance
324 and thus their selective potential for the species has already been shown (Ristola *et al.*, 1999; Kraak
325 *et al.*, 2000; Pfenninger & Nowak, 2008; Nemec *et al.*, 2012, 2013). Even though some parameters
326 showed seasonal changes, these were either overlain by long-term trends or were minor in
327 comparison to the observed changes that did not seem to follow any regular pattern. In
328 consequence, the selective regime as a whole defined by this physico-chemical parameter set was at
329 no point in time identical or even similar to any other period surveyed. Moreover, only a small subset
330 of the potentially selectively relevant biotic and abiotic parameters was measured. For example,
331 predation (Correia *et al.*, 2005) and other intra- and interspecific ecological interactions that are
332 known to play an important role for the fitness of *C. riparius* (van de Bund & Davids, 1993; Hooper *et*
333 *al.*, 2003) were not taken into account. It is therefore reasonable to assume that an unknown, but
334 much larger number of selective factors is simultaneously, yet in strength and direction more or less
335 independently, acting on this population. The local habitat is therefore probably conforming to the
336 multi-scale theory of the environment (Bell, 2010).

337 *Continuous phenotypic evolution with frequent changes in direction*

338 The measured phenotypes of the natural population varied significantly among sampling dates and
339 inversed the direction of change repeatedly and independently across traits. To distinguish between
340 phenotypic plasticity and adaptation, we measured the traits in the F1 generation under standard
341 laboratory conditions, which may be viewed as too few to exclude imprinting effects (Glastad *et al.*,
342 2019). The laboratory conditions, however, are themselves not selectively neutral for field
343 populations (Pfenninger & Foucault, 2020). Given the propensity for rapid adaptation in the
344 laboratory, particularly in the first few generations when confronted with a new stressor (e.g. (Doria
345 *et al.*, 2022a, 2022b), it was necessary to balance between these two pitfalls.

346 We observed strong evolutionary responses, with per generation rates that were in range of those
347 observed for insects in laboratory experiments (Hoffmann & Ross, 2018) or in the semi-natural
348 setting of (Rudman *et al.*, 2021). Because there were frequent changes in the direction of change, the
349 chosen test interval was crucial; as in the latter study, the choice of another time scale could have
350 suggested no phenotypic change at all.

351 Most importantly for the diagnosis of adaptive tracking was that phenotypic evolution occurred on
352 the same temporal scale as the environmental change. However, we did not test for a direct link
353 between any environmental parameter and a phenotypic trait, because i) the measured traits are
354 rather highly inclusive fitness components, thus integrating the influence of many lower level traits,
355 ii) transient, short term extreme events were not recorded by the long-term averages, but are known
356 to exert important selective pressure (Pfenninger *et al.*, 2022). All measured traits have strong links
357 to fitness, which also varied over the monitored period. This concurred to selective dynamic patterns
358 generally known from natural populations (Kingsolver *et al.*, 2012).

359 *Rapid and pervasive selective genomic evolution*

360 The analysis of population genomic time series showed that tens of thousands loci showed signs of at
361 least one selection-driven change in allele frequency across sampling periods, corresponding to less
362 than 30 generations. Rapid and substantial changes in allele frequencies were observed throughout

363 the genome. As the chosen approach accounted for drift and sampling variance (Taus *et al.*, 2017),
364 and immigration was unlikely to change allele frequencies noticeably (Foucault *et al.*, 2019a), the
365 observed significant changes are likely due to selection alone. This supports the increasing
366 observations of rapid adaptive change in natural populations (e.g. (Torda *et al.*, 2017; Dayan *et al.*,
367 2019). The observation that the standard deviation of the selection coefficients, an equivalent to
368 selection intensity, was much larger than the respective mean (0.68 vs. 0.30) proved substantial
369 changes in magnitude and frequent reversals in the direction of selection. The acting selection
370 regime thus corresponded to the multi-scale model of fluctuating selection advocated by (Bell, 2010).

371 The propensity to rapid adaptation with simultaneous preservation of genetic variation in *C. riparius*
372 is thus probably due to an interplay of genomic, life cycle and demographic traits of the species. On
373 the genomic level, the low observed mean LD resulted in a highly fragmented haplotype structure,
374 comparable in scale to other insects like *Drosophila* (Feder *et al.*, 2012). A short range haplotype
375 structure is a precondition for the observed short distance between haplotypes responding to
376 selection. Since only haplotypes with more than a single SNP were considered, this may even present
377 an underestimate, because ancient selected polymorphisms may very well be completely separated
378 from their background by recombination (Pfenninger *et al.*, 2022). In some instances, even different
379 parts of the same gene followed different evolutionary trajectories. The observed fine-scaled
380 selective response to independently fluctuating environmental parameters requires that many
381 different recombinational variants are permanently present in the population. This may be one
382 reason for the gross overproduction of offspring in the species (Foucault *et al.*, 2019b). A large
383 offspring number implies a respectively large number of independent recombinational events,
384 creating a wide variety of new genotypes from which to select. Together with the large, fluctuating
385 demographic and effective population size, the preconditions for rapid, fine-scaled and variable
386 evolutionary reaction to fluctuating changes in the selective regime are therefore given.

387 *The number of temporal evolutionary trajectories is limited but dynamic*

388 In comparison to the huge number of potentially independent loci in terms of physical linkage
389 reacting to selection, the number of statistically distinguishable evolutionary trajectories was quite
390 limited (46). Despite expected trade-offs and pleiotropy between loci (Li *et al.*, 2019), this suggested
391 that rather the number of detectable selection pressures was limited than the capacity of the
392 population to follow them. That the majority of genes was not measurably affected by selection
393 suggested unused adaptive potential, but could also be due to small effect size loci that did not reach
394 statistical significance in the present analysis.

395 While the order of magnitude of estimated effectively acting selection pressures is certainly correct,
396 the exact value may not be. On the one hand, the statistically derived clustering threshold was
397 possibly too rigid and therefore distinguished too many clusters, as indicated by the correlation of
398 some very similar MHT clusters (MHT21, MHT22 and MHT17, MHT18, MHT19) to the same
399 environmental variables (Fig. 3). On the other hand, in longer time series other selection pressures
400 could have elicited additional statistically detectable MHT or split co-varying but distinctive selection
401 pressures into distinguishable haplotype trajectories, thus increasing the estimate of acting selective
402 agents. A hint in this direction was the increase from 36 distinguishable MHTs in a preliminary
403 analysis after five temporal samplings (data not shown) to 46 after six. It was therefore possible that
404 the number of selection pressures the population can effectively follow independently within few
405 generations may be finally limited, but could be different than estimated here. However, general
406 conclusions will require the application of the framework presented here to more populations over
407 more generations and different species.

408 Changes in intensity and direction of MHTs were observed frequently, thus corroborating the results
409 gained from phenotypic traits. The number of haplotypes that showed a continuous increase or
410 decline in allele frequency over the monitored period were relatively limited (MHT4, 724 loci),
411 suggesting that adaptation proceeds mainly by short time scale tracking of varying selection
412 pressures and not by slow fixation of alleles.

413 As expected from studies on *Drosophila* (Bergland *et al.*, 2014), MHT patterns reflecting seasonal
414 variation were identified. MHT38, highly correlated to temperature and MHT40 showed respective
415 patterns, accounting for about 1.2% of all selected haplotypes. This is in the range found for seasonal
416 fluctuations of allele frequencies in *Drosophila* (Bergland *et al.*, 2014; Machado *et al.*, 2021).
417 However, compared to the high variability of the remaining MHT patterns, the seasonal variations in
418 temperature, precipitation, resource availability etc. were surprisingly of relatively minor
419 importance.

420 *Environmental associations and functional gene enrichments of MHTs*

421 The number of MHTs in each cluster was highly different, ranging from a few to many thousands. On
422 average, many independent loci were therefore involved in the same adaptive response, which is
423 typical for polygenic traits (Jain & Stephan, 2017). However, enrichment analyses in the GO category
424 Biological Process for genes overlapping with haplotypes from respective MHT clusters rarely yielded
425 clearly interpretable patterns. In some instances, hypotheses on the acting selection pressures could
426 be gained from the enrichment analyses. In particular MHT4 suggested a biological interaction,
427 perhaps in defence to parasites. Immune genes adaptively tracking the abundance of potential
428 pathogens over seasons were also found in wild *D. melanogaster* populations (Behrman *et al.*, 2018).
429 Another interesting set of enriched genes associated with porphyrin containing pigment metabolism
430 was found in MHT36. The most important pigments in Chironomids are hemoglobins, giving the
431 characteristic red colour to these midges (also called "bloodworms"). They play an important role in
432 hypoxia/anoxia (Grazioli *et al.*, 2016) and are negatively influenced in their function by nitrite (Ha &
433 Choi, 2008). It was thus not surprising that the highest correlations of this MHT were to oxygen (r =
434 0.74) and NO_2 (r = 0.78), respectively. Less than a quarter of the MHT patterns were highly (> 0.9)
435 correlated with the few measured environmental parameters, indicating that only a small proportion
436 of selectively relevant parameters were measured. Some correlations suggestively matched the
437 inferred functions from the GO enrichment analysis. MHT39, enriched for genes involved in *nitric-*
438 *oxide synthase inhibitor activity,* was highly correlated to NO_2, underlining the importance of

439 nitrogen metabolism for the species (Pfenninger & Nowak, 2008). Another match was found for
440 MHT21, strongly associated with biological oxygen demand, which reflects the availability of organic
441 matter in the stream, an important food source for the midges (Ristola *et al.*, 1999). Among the GO
442 terms enriched in this MHT, *carbohydrate metabolism* was found, insinuating an adaptive reaction to
443 the food availability.

444 *Adaptive tracking of environmental changes*

445 The observed substantial rapid phenotypic and selectively driven genomic evolution with changing
446 signs on the same time scale as putatively selectively relevant environmental variation strongly
447 suggested that the natural *C. riparius* population studied here adaptively tracked their environment.
448 This implies the existence of abundant, unlinked genetic variation under fluctuating selection. In
449 classical population genetic predictions, adaptive tracking as observed here is viewed as unlikely to
450 evolve, because fluctuating selection should rapidly eliminate genetic variation (Hedrick, 2006).
451 Several recent models, however, have called these predictions into question. It was shown that in a
452 multivoltine species, adaptive tracking is more likely to evolve than phenotypic plasticity or bet-
453 hedging (Botero *et al.*, 2015). Dominance shifts of adaptive alleles (Wittmann *et al.*, 2017) and boom-
454 bust cycles (Bertram & Masel, 2019) can additionally contribute to the maintenance of genetic
455 variation and are probably common in species satisfying these conditions (Kain *et al.*, 2015).

456 Species following such an evolutionary regime should be able to cope also with long term trends as
457 imposed by global change. The next logical step will be to increase the temporal sampling and
458 analyse the spatial dimension. This promises to obtain statistically reliable associations whose
459 functional causalities may then be experimentally validated (but see (Pfenninger & Foucault, 2020)).

460 *Conclusion*

461 The present study suggested that natural populations can adaptively track the environmental
462 changes in their habitat. It confirms thus findings of a recent experimental study on *Drosophila*
463 (Rudman *et al.*, 2021), indicating the relevance of the process for real world populations. Pending

further support from additional taxa, these studies provide support for the idea that evolutionary and ecological time scales may not differ at all (Hairston Jr *et al.*, 2005). In addition, the rapid and pervasive action of natural selection on the genomic level challenges long-standing population genetic paradigms (Messer *et al.*, 2016; Kern & Hahn, 2018).

Beyond these important scientific questions, the presented framework opens the possibility to use population genomic time series for applied functional environmental monitoring (Pfenninger & Bálint, 2022). While currently rather the presence or absence of species is used to evaluate the state of environments, the monitoring of selective changes associated with certain anthropogenic or environmental factors could serve as an early warning system before any community change would be visible. Such knowledge may soon be of crucial importance to direct biodiversity conservation and mitigation strategies in a rapidly changing world.

Author Contributions

Conceptualization MP, Methodology Development MP, Software Programming MP, Validation MP, Formal Analysis MP, Investigation QF, MP, Resources MP, Data Curation MP, Writing – Original DrMHT Preparation MP, Writing – Review & Editing Preparation QF, MP, Visualization Preparation MP, Supervision MP, Project Administration Management MP, Funding Acquisition MP.

Acknowledgements

We thank Andreas Wieser for help with sampling and the Abwasserverband Freigericht for generously providing the environmental Hasselbach data. The work was funded by DFG (grant PF390/8-1).

Declaration of interests

The authors declare no conflict of interest.

Data and Code Availability

Sequencing data is publicly available on ENA (project ERP115516, samples ERS4040036-ERS4040041).

Core scripts and sync-files were made available on DRYAD (doi.org/10.5061/dryad.fxpnvx0nd).

References

Abdul-Rahman, F., Tranchina, D. & Gresham, D. (2021) Fluctuating Environments Maintain Genetic Diversity through Neutral Fitness Effects and Balancing Selection. *Molecular Biology and Evolution*, **38**, 4362–4375.

Alexa, A. & Rahnenführer, J. (2016) Gene set enrichment analysis with topGO. R package version 2.24. 0.

Bååth, R. (2014) Bayesian first aid: A package that implements Bayesian alternatives to the classical*. test functions in R. *Proceedings of useR*, **2014**, 2.

Barghi, N., Hermisson, J. & Schlötterer, C. (2020) Polygenic adaptation: a unifying framework to understand positive selection. *Nature Reviews Genetics*, **21**, 769–781.

Barton, N.H. & Keightley, P.D. (2002) Understanding quantitative genetic variation. *Nature Reviews Genetics*, **3**, 11–21.

Behrman, E.L., Howick, V.M., Kapun, M., Staubach, F., Bergland, A.O., Petrov, D.A., *et al.* (2018) Rapid seasonal evolution in innate immunity of wild Drosophila melanogaster. *Proceedings of the Royal Society B: Biological Sciences*, **285**, 20172599.

Bell, G. (2010) Fluctuating selection: the perpetual renewal of adaptation in variable environments. *Philosophical Transactions of the Royal Society B: Biological Sciences*, **365**, 87–97.

Bergland, A.O., Behrman, E.L., O'Brien, K.R., Schmidt, P.S. & Petrov, D.A. (2014) Genomic evidence of rapid and stable adaptive oscillations over seasonal time scales in Drosophila. *PLoS genetics*, **10**, e1004775.

Bertram, J. & Masel, J. (2019) Different mechanisms drive the maintenance of polymorphism at loci subject to strong versus weak fluctuating selection. *Evolution*, **73**, 883–896.

Bitter, M.C., Kapsenberg, L., Gattuso, J.-P. & Pfister, C.A. (2019) Standing genetic variation fuels rapid adaptation to ocean acidification. *Nature communications*, **10**, 1–10.

Boag, P.T. & Grant, P.R. (1981) Intense natural selection in a population of Darwin's finches (Geospizinae) in the Galapagos. *Science*, **214**, 82–85.

Bolger, A.M., Lohse, M. & Usadel, B. (2014) Trimmomatic: a flexible trimmer for Illumina sequence data. *Bioinformatics*, **30**, 2114–2120.

Botero, C.A., Weissing, F.J., Wright, J. & Rubenstein, D.R. (2015) Evolutionary tipping points in the capacity to adapt to environmental change. *Proceedings of the National Academy of Sciences*, **112**, 184–189.

Bund, W.J. van de & Davids, C. (1993) Complex relations between freshwater macro-and meiobenthos: interactions between Chironomus riparius and Chydorus piger. *Freshwater Biology*, **29**, 1–6.

Correia, A.M., Bandeira, N. & Anastácio, P.M. (2005) Predator–prey interactions of Procambarus clarkii with aquatic macroinvertebrates in single and multiple prey systems. *Acta Oecologica*, **28**, 337–343.

Croze, M., Wollstein, A., Božičević, V., Živković, D., Stephan, W. & Hutter, S. (2017) A genome-wide scan for genes under balancing selection in Drosophila melanogaster. *BMC Evolutionary Biology*, **17**, 1–12.

Dayan, D.I., Du, X., Baris, T.Z., Wagner, D.N., Crawford, D.L. & Oleksiak, M.F. (2019) Population genomics of rapid evolution in natural populations: polygenic selection in response to power station thermal effluents. *BMC evolutionary biology*, **19**, 1–20.

532 Doria, H.B., Caliendo, C., Gerber, S. & Pfenninger, M. (2022a) Photoperiod is an important seasonal
533 selection factor in Chironomus riparius (Diptera: Chironomidae). *Biological Journal of the Linnean*
534 *Society*, **135**, 277–290.
535 Doria, H.B., Hannappel, P. & Pfenninger, M. (2022b) Whole genome sequencing and RNA-seq
536 evaluation allowed to detect Cd adaptation footprint in Chironomus riparius. *Science of The Total*
537 *Environment*, 152843.
538 Feder, A.F., Petrov, D.A. & Bergland, A.O. (2012) LDx: estimation of linkage disequilibrium from high-
539 throughput pooled resequencing data. *PloS one*, **7**, e48588.
540 Foucault, Q., Wieser, A., Heumann-Kiesler, C., Diogo, J., Cocchiararo, B., Nowak, C., *et al.* (2019a) An
541 experimental assessment of reproductive isolation and its consequences for seasonal hybridization
542 dynamics. *Biological Journal of the Linnean Society*, **126**, 327–337.
543 Foucault, Q., Wieser, A., Waldvogel, A.M., Feldmeyer, B. & Pfenninger, M. (2018) Rapid adaptation to
544 high temperatures in Chironomus riparius. *Ecology and Evolution*, **8**, 12780–12789.
545 Foucault, Q., Wieser, A., Waldvogel, A.-M. & Pfenninger, M. (2019b) Establishing laboratory cultures
546 and performing ecological and evolutionary experiments with the emerging model species
547 Chironomus riparius. *Journal of Applied Entomology*, **143**, 584–592.
548 Franssen, S.U., Barton, N.H. & Schlötterer, C. (2016) Reconstruction of haplotype-blocks selected
549 during experimental evolution. *Molecular biology and evolution*, msw210.
550 Glastad, K.M., Hunt, B.G. & Goodisman, M.A.D. (2019) Epigenetics in Insects: Genome Regulation and
551 the Generation of Phenotypic Diversity. *Annual Review of Entomology*, **64**, 185–203.
552 Grant, B.R. & Grant, P.R. (1989) Natural selection in a population of Darwin's finches. *The American*
553 *Naturalist*, **133**, 377–393.
554 Grazioli, V., Rossaro, B., Parenti, P., Giacchini, R. & Lencioni, V. (2016) Hypoxia and anoxia effects on
555 alcohol dehydrogenase activity and hemoglobin content in Chironomus riparius Meigen, 1804.
556 *Journal of Limnology*, **75**.
557 Ha, M.-H. & Choi, J. (2008) Effects of environmental contaminants on hemoglobin of larvae of aquatic
558 midge, Chironomus riparius (Diptera: Chironomidae): A potential biomarker for ecotoxicity
559 monitoring. *Chemosphere*, **71**, 1928–1936.
560 Hairston Jr, N.G., Ellner, S.P., Geber, M.A., Yoshida, T. & Fox, J.A. (2005) Rapid evolution and the
561 convergence of ecological and evolutionary time. *Ecology Letters*, **8**, 1114–1127.
562 Haldane, J.B.S. (1949) Suggestions as to Quantitative Measurement of Rates of Evolution. *Evolution*,
563 **3**, 51–56.
564 Hammer, Ø., Harper, D.A.T. & Ryan, P.D. (2001) PAST-Palaeontological statistics. *Palaeontologia*
565 *electronica*, **4**, 1–9.
566 Hedrick, P.W. (2006) Genetic polymorphism in heterogeneous environments: the age of genomics.
567 *Annu. Rev. Ecol. Evol. Syst.*, **37**, 67–93.
568 Hendry, A.P. (2019) A critique for eco-evolutionary dynamics. *Functional Ecology*, **33**, 84–94.
569 Hoffmann, A.A. & Ross, P.A. (2018) Rates and Patterns of Laboratory Adaptation in (Mostly) Insects.
570 *Journal of Economic Entomology*, **111**, 501–509.
571 Hooper, H.L., Sibly, R.M., Hutchinson, T.H. & Maund, S.J. (2003) The influence of larval density, food
572 availability and habitat longevity on the life history and population growth rate of the midge
573 Chironomus riparius. *Oikos*, **102**, 515–524.
574 Jain, K. & Stephan, W. (2017) Modes of rapid polygenic adaptation. *Molecular biology and evolution*,
575 **34**, 3169–3175.
576 Kain, J.S., Zhang, S., Akhund-Zade, J., Samuel, A.D., Klein, M. & Bivort, B.L. de. (2015) Variability in
577 thermal and phototactic preferences in Drosophila may reflect an adaptive bet-hedging strategy.
578 *Evolution*, **69**, 3171–3185.
579 Kern, A.D. & Hahn, M.W. (2018) The neutral theory in light of natural selection. *Molecular biology*
580 *and evolution*, **35**, 1366–1371.
581 Kimura, J.F.C. (1970) *Introduction to Population Genetics Theory*. Harper & Row Publishers.
582 King, J.G. & Hadfield, J.D. (2019) The evolution of phenotypic plasticity when environments fluctuate
583 in time and space. *Evolution Letters*, **3**, 15–27.

Kingsolver, J.G., Diamond, S.E., Siepielski, A.M. & Carlson, S.M. (2012) Synthetic analyses of phenotypic selection in natural populations: lessons, limitations and future directions. *Evolutionary Ecology*, **26**, 1101–1118.

Kofler, R., Orozco-terWengel, P., De Maio, N., Pandey, R.V., Nolte, V., Futschik, A., *et al.* (2011a) PoPoolation: a toolbox for population genetic analysis of next generation sequencing data from pooled individuals. *PloS one*, **6**, e15925.

Kofler, R., Pandey, R.V. & Schlötterer, C. (2011b) PoPoolation2: identifying differentiation between populations using sequencing of pooled DNA samples (Pool-Seq). *Bioinformatics*, **27**, 3435–3436.

Kraak, M.H., Stuijfzand, S.C. & Admiraal, W. (2000) Interaction between organic matter and toxicants in polluted river water: beneficial and inhibiting effects on the midge Chironomus riparius.

Li, H. & Durbin, R. (2009) Fast and accurate short read alignment with Burrows–Wheeler transform. *bioinformatics*, **25**, 1754–1760.

Li, H., Handsaker, B., Wysoker, A., Fennell, T., Ruan, J., Homer, N., *et al.* (2009) The sequence alignment/map format and SAMtools. *Bioinformatics*, **25**, 2078–2079.

Li, Y., Petrov, D.A. & Sherlock, G. (2019) Single nucleotide mapping of trait space reveals Pareto fronts that constrain adaptation. *Nature ecology & evolution*, **3**, 1539–1551.

Machado, H.E., Bergland, A.O., Taylor, R., Tilk, S., Behrman, E., Dyer, K., *et al.* (2021) Broad geographic sampling reveals the shared basis and environmental correlates of seasonal adaptation in Drosophila. *Elife*, **10**, e67577.

Margres, M.J., Wray, K.P., Hassinger, A.T., Ward, M.J., McGivern, J.J., Moriarty Lemmon, E., *et al.* (2017) Quantity, not quality: rapid adaptation in a polygenic trait proceeded exclusively through expression differentiation. *Molecular biology and evolution*, **34**, 3099–3110.

Marrot, P., Garant, D. & Charmantier, A. (2017) Multiple extreme climatic events strengthen selection for earlier breeding in a wild passerine. *Philosophical Transactions of the Royal Society B: Biological Sciences*, **372**, 20160372.

Matuszewski, S., Hermisson, J. & Kopp, M. (2015) Catch me if you can: adaptation from standing genetic variation to a moving phenotypic optimum. *Genetics*, **200**, 1255–1274.

Messer, P.W., Ellner, S.P. & Hairston, N.G. (2016) Can Population Genetics Adapt to Rapid Evolution? *Trends in Genetics*, **32**, 408–418.

Messer, P.W. & Petrov, D.A. (2013) Population genomics of rapid adaptation by soft selective sweeps. *Trends in ecology & evolution*, **28**, 659–669.

Nemec, S., Heß, M., Nowak, C. & Pfenninger, M. (2012) Experimental evidence for niche segregation in a sister species pair of non-biting midges. *Hydrobiologia*, **691**, 203–212.

Nemec, S., Patel, S., Nowak, C. & Pfenninger, M. (2013) Evolutionary determinants of population differences in population growth rate$\times$ habitat temperature interactions in Chironomus riparius. *Oecologia*, **172**, 585–594.

Oppold, A.M., Pedrosa, J.A.M., Bálint, M., Diogo, J.B., Ilkova, J., Pestana, J.L.T., *et al.* (2016) Support for the evolutionary speed hypothesis from intraspecific population genetic data in the non-biting midge chironomus riparius. *Proceedings of the Royal Society B: Biological Sciences*, **283**.

Pfenninger, M. & Bálint, M. (2022) On the use of population genomic time series for environmental monitoring. *American Journal of Botany*, in press.

Pfenninger, M. & Foucault, Q. (2020) Genomic processes underlying rapid adaptation of a natural Chironomus riparius population to unintendedly applied experimental selection pressures. *Molecular Ecology*, **29**, 536–548.

Pfenninger, M., Foucault, Q., Waldvogel, A.-M. & Feldmeyer, B. (2022) *Selective effects of a short transient environmental fluctuation on a natural population* (preprint). Evolutionary Biology.

Pfenninger, M. & Nowak, C. (2008) Reproductive isolation and ecological niche partition among larvae of the morphologically cryptic sister species Chironomus riparius and C. piger. *PLoS One*, **3**, e2157.

Ristola, T., Pellinen, J., Ruokolainen, M., Kostamo, A. & Kukkonen, J.V. (1999) Effect of sediment type, feeding level, and larval density on growth and development of a midge (Chironomus riparius). *Environmental Toxicology and Chemistry: An International Journal*, **18**, 756–764.

Rozas, J., Ferrer-Mata, A., Sánchez-DelBarrio, J.C., Guirao-Rico, S., Librado, P., Ramos-Onsins, S.E., *et al.* (2017) DnaSP 6: DNA sequence polymorphism analysis of large data sets. *Molecular biology and evolution*, **34**, 3299–3302.

Rudman, S.M., Barbour, M.A., Csilléry, K., Gienapp, P., Guillaume, F., Hairston Jr, N.G., *et al.* (2018) What genomic data can reveal about eco-evolutionary dynamics. *Nature Ecology & Evolution*, **2**, 9–15.

Rudman, S.M., Greenblum, S.I., Rajpurohit, S., Betancourt, N.J., Hanna, J., Tilk, S., *et al.* (2021) Direct observation of adaptive tracking on ecological timescales in Drosophila.

Schmidt, H., Hellmann, S.L., Waldvogel, A.-M., Feldmeyer, B., Hankeln, T. & Pfenninger, M. (2020) A high-quality genome assembly from short and long reads for the non-biting midge Chironomus riparius (Diptera). *G3: Genes, Genomes, Genetics*, **10**, 1151–1157.

Siepielski, A.M., DiBattista, J.D. & Carlson, S.M. (2009) It's about time: the temporal dynamics of phenotypic selection in the wild. *Ecology letters*, **12**, 1261–1276.

Sjölander, A. & Vansteelandt, S. (2019) Frequentist versus Bayesian approaches to multiple testing. *European journal of epidemiology*, **34**, 809–821.

Taus, T., Futschik, A. & Schlötterer, C. (2017) Quantifying selection with pool-seq time series data. *Molecular biology and evolution*, **34**, 3023–3034.

Torda, G., Donelson, J.M., Aranda, M., Barshis, D.J., Bay, L., Berumen, M.L., *et al.* (2017) Rapid adaptive responses to climate change in corals. *Nature Climate Change*, **7**, 627–636.

Van der Auwera, G.A., Carneiro, M.O., Hartl, C., Poplin, R., Del Angel, G., Levy-Moonshine, A., *et al.* (2013) From FastQ data to high-confidence variant calls: the genome analysis toolkit best practices pipeline. *Current protocols in bioinformatics*, **43**, 11–10.

Vander Wal, E., Garant, D., Festa-Bianchet, M. & Pelletier, F. (2013) Evolutionary rescue in vertebrates: evidence, applications and uncertainty. *Philosophical Transactions of the Royal Society B: Biological Sciences*, **368**, 20120090.

Villemereuil, P. de, Charmantier, A., Arlt, D., Bize, P., Brekke, P., Brouwer, L., *et al.* (2020) Fluctuating optimum and temporally variable selection on breeding date in birds and mammals. *Proceedings of the National Academy of Sciences*, **117**, 31969–31978.

Waldvogel, A.M., Wieser, A., Schell, T., Patel, S., Schmidt, H., Hankeln, T., *et al.* (2018) The genomic footprint of climate adaptation in Chironomus riparius. *Molecular Ecology*, **27**, 1439–1456.

Wittmann, M.J., Bergland, A.O., Feldman, M.W., Schmidt, P.S. & Petrov, D.A. (2017) Seasonally fluctuating selection can maintain polymorphism at many loci via segregation lift. *Proceedings of the National Academy of Sciences*, **114**, E9932–E9941.

Yang, J.I., Li, W.-R., Lv, F.-H., He, S.-G., Tian, S.-L., Peng, W.-F., *et al.* (2016) Whole-genome sequencing of native sheep provides insights into rapid adaptations to extreme environments. *Molecular biology and evolution*, **33**, 2576–2592.

Zong, S.-B., Li, Y.-L. & Liu, J.-X. (2021) Genomic architecture of rapid parallel adaptation to fresh water in a wild fish. *Molecular biology and evolution*, **38**, 1317–1329.

Figures

Figure 1. PCA on seasonal physico-chemical water parameters in the natural population for the decade from 2009-2018. Shown are the first two axes, accounting for 82.2% of environmental variation. Periods after which phenotypic and genomic assessments of the population were performed are indicated in bold. The temporal trajectory of the environmental conditions are indicated by arrows connecting consecutive periods.

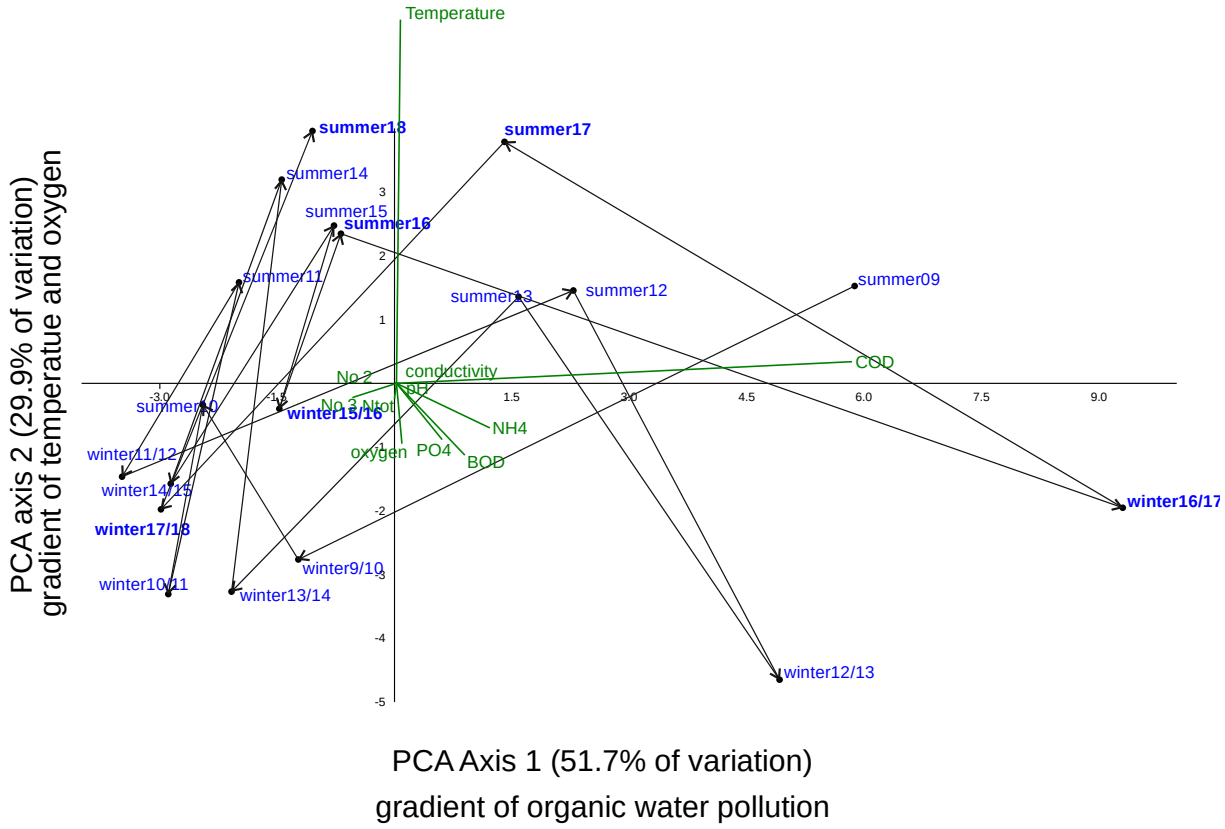

Figure 2. Development of phenotypic traits and population fitness over time in the natural population. A) Developmental time measured as EmT50. B) Mortality measured as proportion of emerged individuals. C) Fecundity as viable eggs per female. D) Population growth rate per day as integrative measure of population fitness.

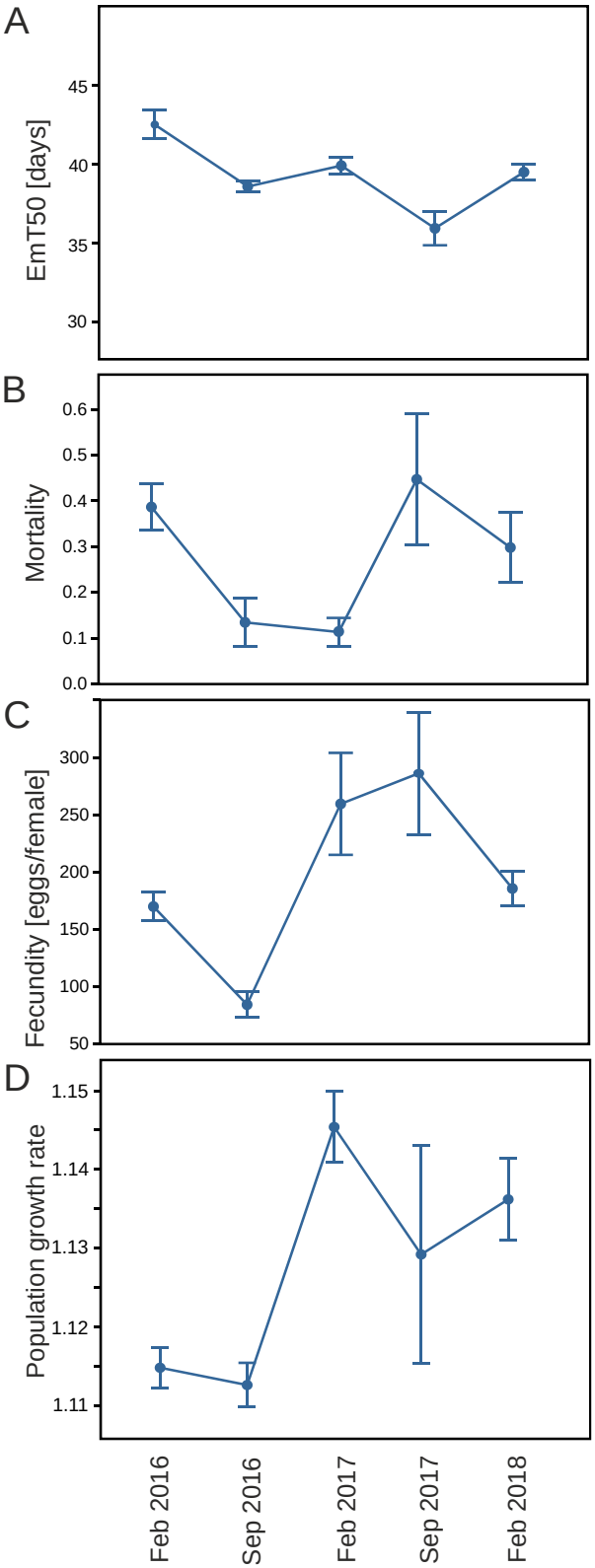

Figure 3. Temporal dynamics and complexity of allele frequencies trajectories with signs of selection. The left side of the panel shows a UPGMA-dendrogram on the pairwise distance (1 - correlation coefficients) of all 35,574 haplotype MHTs with at least one significant AFC. The hatched vertical line presents the inferred clustering threshold of 0.25. The right side of the panel shows the MHTs for each cluster. For better visibility and comparability, the individual MHTs in each cluster were polarised into the same direction and normalised by substracting the respective mean.

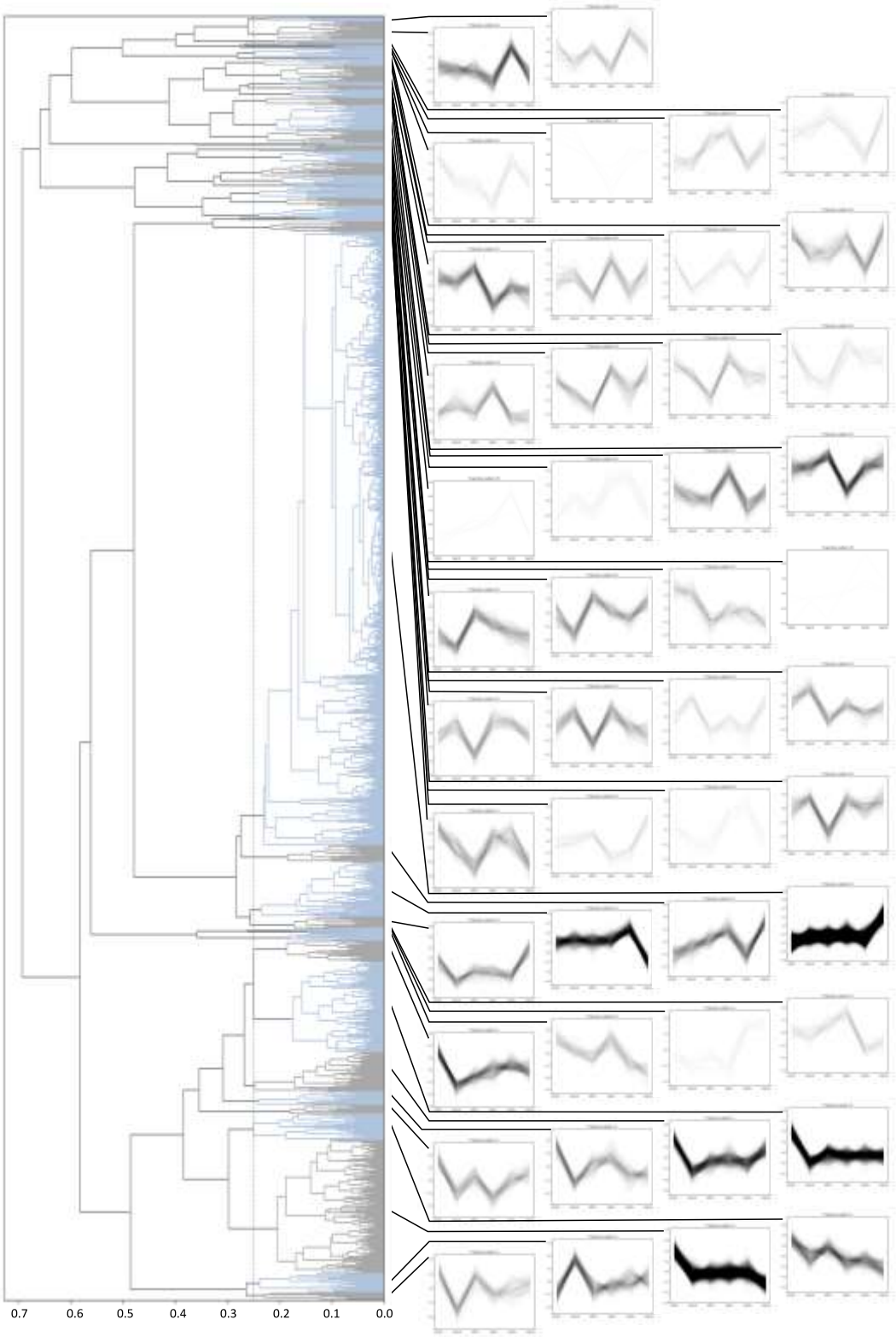

Fig 3. Correlations between measured environmental parameters and MHTs. Shown are only associations with a posterior credibility > 95%. Please note that the direction of the correlation depends on the arbitrary polarisation of the alleles in the allele frequency trajectory.

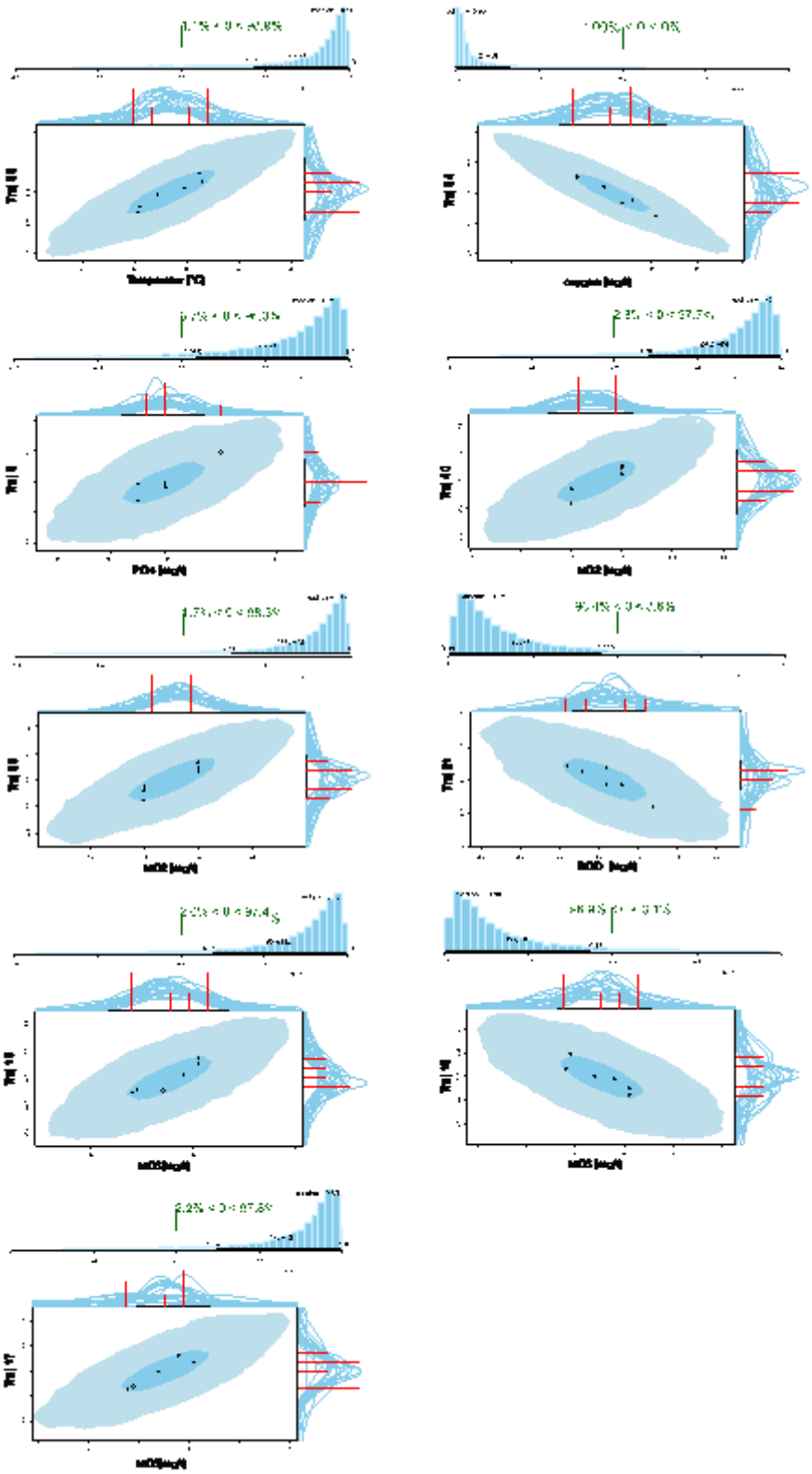

SUPPLEMENT

SUPPL. RESULTS

Table 1. Results of two way ANOVA on fitness data of the field population to three experimental temperatures (14°C, 20°C, 26°C) at 5 different sampling dates (Feb. 16, Sept. 16, Feb. 17, Sep. 17, Feb. 18).

Factor	Sum of sqrs	d.f.	Mean square	F	p (same)
Sampling date	0.037	4	0.009	9.509	5.07E-06
Exp. Temp	0.527	2	0.263	269.6	1.05E-30
Interaction	0.028	8	0.004	3.631	0.001668
Within	0.059	60	0.001		
Total	0.651	74			

Table 2. Frequency distribution of MHT cluster patterns, environmental parameter with correlation coefficient > 0.9, number of genes affected and first four most significantly enriched GFO terms for the 46 observed MHT clusters.

Cluster ID	**N MHT**	**Env. Parameter r r > 0.9**	**N genes**	**Significant GO Terms**			
1	244	-	72	0045454, cell redox homeostasis, 41, 2, 0.28, 0.031	0006606, protein import into nucleus, 6, 1, 0.04, 0.040	0006355, regulation of transcription, DNA-templat..., 322, 6, 2.2, 0.040	0007165, signal transduction, 397, 8, 2.71, 0.046
2	521	-	152	0007205, protein kinase C-activating G protein-co..., 5, 2, 0.06, 0.0016	0007017, microtubule-based process, 64, 4, 0.82, 0.0163	0007264, small GTPase mediated signal transductio..., 55, 3, 0.7, 0.0233	
3	3943	PO_4	1126	0006811, ion transport, 300, 33, 22.94, 2.7e-05	0007156, homophilic cell adhesion via plasma memb..., 25, 7, 1.91, 0.0021	0006836, neurotransmitter transport, 14, 5, 1.07, 0.0028	0042737, drug catabolic process, 11, 4, 0.84, 0.0072
4	742	-	262	0051704, multi-organism process, 7, 2, 0.14, 0.0081	0006952, defense response, 9, 2, 0.18, 0.0136	0055085, transmembrane transport, 439, 16, 8.99, 0.0226	0006816, calcium ion transport, 17, 2, 0.22, 0.0372
5	289	-	94	0006355, regulation of transcription, DNA-templat..., 322, 7, 2.12, 0.012	0007268, chemical synaptic transmission, 6, 1, 0.04, 0.039		
6	352	-	111	0055114, oxidation-reduction process, 433, 10, 4.14, 0.0099	0009116, nucleoside metabolic process, 23, 2, 0.22, 0.0199	0072522, purine-containing compound biosynthetic ..., 58, 2, 0.55, 0.0373	0006120, mitochondrial electron transport, NADH t..., 5, 1, 0.05, 0.0469
7	1183	-	354	0035556, intracellular signal transduction,	0007275, multicellular organism development,	0006836, neurotransmitter transport, 14, 3, 0.38, 0.0055	0042246, tissue regeneration,

				132, 11, 3.54, 0.0030	25, 4, 0.67, 0.0040		5, 2, 0.13, 0.0068
8	2611	-	816	0015698, inorganic anion transport, 15, 5, 0.93, 0.00043	0006811, ion transport, 300, 32, 18.57, 0.00378	0055085, transmembrane transport, 439, 41, 27.17, 0.01175	0006629, lipid metabolic process, 189, 13, 11.7, 0.02091
9	660	-	215	0007156, homophilic cell adhesion via plasma memb..., 25, 4, 0.44, 0.00087	0034220, ion transmembran e transport, 88, 4, 1.56, 0.01161	3, 0009072, aromatic amino acid family metabolic pro..., 13, 2, 0.23, 0.02137	0055085, transmembran e transport, 439, 16, 7.79, 0.02999
10	208	-	61	0007264, small GTPase mediated signal transductio..., 55, 2, 0.25, 0.025	0006207, 'de novo' pyrimidine nucleobase biosynth..., 6, 1, 0.03, 0.027		
11	29	-	13	-			
12	102	-	24	0032269, negative regulation of cellular protein ..., 6, 1, 0.01, 0.012	0006417, regulation of translation, 9, 1, 0.02, 0.018	0006413, translational initiation, 13, 1, 0.03, 0.026	2000113, negative regulation of cellular macromol..., 14, 1, 0.03, 0.028
13	355	-	136	0007165, signal transduction, 397, 14, 4.61, 0.00043			
14	1580	-	569	0007156, homophilic cell adhesion via plasma memb..., 25, 6, 1.15, 0.00076	0007155, cell adhesion, 49, 11, 2.26, 0.00373	0035556, intracellular signal transduction, 132, 10, 6.1, 0.02015	0006012, galactose metabolic process, 6, 2, 0.28, 0.02816
15	514	-	175	0007156, homophilic cell adhesion via plasma memb..., 25, 3, 0.4, 0.0069	0006979, response to oxidative stress, 22, 2, 0.35, 0.0471		
16	17914	-	4831	0055085, transmembrane transport, 439, 202, 159.22, 1.5e-05	0007166, cell surface receptor signaling pathway, 53, 32, 19.22, 9.9e-05	0007156, homophilic cell adhesion via plasma memb..., 25, 18, 9.07, 0.00029	0006811, ion transport, 300, 139, 108.81, 0.00059
17	333	NO_3	106	0006813, potassium ion transport, 46, 5, 0.33, 0.0016	0071805, potassium ion transmembran e transport, 11, 2, 0.08, 0.0027	0051260, protein homoolimerizatio n, 14, 2, 0.1, 0.0044	0010646, regulation of cell communicatio n, 53, 3, 0.39, 0.0273
18	66	NO_3	19	0006364, rRNA processing, 20, 1, 0.02, 0.023			
19	25	NO_3	6	0009072, aromatic amino acid family metabolic pro...,			

				13, 1, 0.01, 0.0088			
20	340	-	100	0007156, homophilic cell adhesion via plasma memb..., 25, 3, 0.19, 0.00079	0006486, protein glycosylation, 36, 2, 0.27, 0.02938	0006072, glycerol-3-phosphate metabolic process, 5, 1, 0.04, 0.03700	
21	242	BOD	83	0005975, carbohydrate metabolic process, 172, 4, 1.21, 0.015			
22	324	BOD	110	0007608, sensory perception of smell, 12, 2, 0.11, 0.0055	0006979, response to oxidative stress, 22, 2, 0.21, 0.0182	0006368, transcription elongation from RNA polyme..., 5, 1, 0.05, 0.0469	
23	67	-	24	0006955, immune response, 6, 1, 0.01, 0.012	0051604, protein maturation, 20, 1, 0.04, 0.040	0018205, peptidyl-lysine modification, 22, 1, 0.05, 0.044	
24	253	-	91	0006979, response to oxidative stress, 22, 2, 0.16, 0.011	0051259, protein complex olimerization, 16, 2, 0.12, 0.014	0055114, oxidation-reduction process, 433, 7, 3.15, 0.033	0005975, carbohydrate metabolic process, 172, 4, 1.25, 0.035
25	392	-	128	0042325, regulation of phosphorylation, 7, 2, 0.07, 0.0093	0006811, ion transport, 300, 8, 2.87, 0.0113	0043086, negative regulation of catalytic activit..., 5, 1, 0.05, 0.0469	0007205, protein kinase C-activating G protein-co..., 5, 1, 0.05, 0.0469
26	325	-	111	0044262, cellular carbohydrate metabolic process, 20, 2, 0.21, 0.018	0007264, small GTPase mediated signal transductio..., 55, 3, 0.58, 0.019	0034220, ion transmembrane transport, 88, 3, 0.92, 0.031	
27	197	-	57	0009395, phospholipid catabolic process, 6, 1, 0.02, 0.023	0007179, transforming growth factor beta receptor..., 7, 1, 0.03, 0.027		
28	3	-	1	-			
29	8	-	4	0007264, small GTPase mediated signal transductio..., 55, 1, 0.03, 0.025			
30	29	-	8	0032012, regulation of ARF protein signal transdu..., 7, 1, 0, 0.0032			
31	406	-	125	0042133, neurotransmitter metabolic	0007205, protein kinase C-activating G		

				process, 8, 2, 0.08, 0.0024	protein-co..., 5, 1, 0.05, 0.0469		
32	697	-	206	0006596, polyamine biosynthetic process, 9, 2, 0.12, 0.0064	0006508, proteolysis, 618, 16, 8.58, 0.0076	0007165, signal transduction, 397, 11, 5.51, 0.0088	0018393, internal peptidyl-lysine acetylation, 9, 2, 0.12, 0.0137
33	230	-	67	0006470, protein dephosphorylatio n, 28, 2, 0.16, 0.011	0007018, microtubule-based movement, 39, 2, 0.22, 0.020	0055085, transmembrane transport, 439, 7, 2.5, 0.035	0034030, ribonucleoside bisphosphate biosynthetic..., 7, 1, 0.04, 0.039
34	222	O_2	81	0007275, multicellular organism development, 25, 2, 0.18, 0.013	1901642, nucleoside transmembran e transport, 5, 1, 0.04, 0.035	0007169, transmembrane receptor protein tyrosine ..., 6, 1, 0.04, 0.042	0046173, polyol biosynthetic process, 6, 1, 0.04, 0.042
35	151	-	44	0007205, protein kinase C-activating G protein-co..., 5, 1, 0.02, 0.020	0005978, glycogen biosynthetic process, 5, 1, 0.02, 0.020	0006207, 'de novo' pyrimidine nucleobase biosynth..., 6, 1, 0.02, 0.024	0006013, mannose metabolic process, 6, 1, 0.02, 0.024
36	71	-	20	0006779, porphyrin-containing compound biosynthet..., 5, 1, 0.01, 0.0091	0046148, pigment biosynthetic process, 7, 1, 0.01, 0.0127	0006629, lipid metabolic process, 189, 2, 0.34, 0.0434	
37	504	-	157	0006979, response to oxidative stress, 22, 4, 0.32, 0.00025	0055114, oxidation-reduction process, 433, 13, 6.31, 0.00833	0006928, movement of cell or subcellular componen..., 41, 3, 0.6, 0.02827	0006813, potassium ion transport, 46, 3, 0.67, 0.02866
38	187	Temp.	60	0007179, transforming growth factor beta receptor..., 7, 1, 0.04, 0.035	0000226, microtubule cytoskeleton organization, 9, 1, 0.05, 0.044		
39	52	NO_2	19	0070588, calcium ion transmembrane transport, 14, 1, 0.01, 0.0095			
40	269	NO_2	90	0007186, G protein-coupled receptor signaling pat..., 137, 4, 0.9, 0.012	0006355, regulation of transcription, DNA-templat..., 322, 6, 2.12, 0.017	1901362, organic cyclic compound biosynthetic pro..., 533, 8, 3.52, 0.027	4, 0008202, steroid metabolic process, 6, 1, 0.04, 0.039
41	52	-	17	0006368, transcription elongation from RNA polyme..., 5, 1, 0, 0.0045	0005975, carbohydrate metabolic process, 172, 2, 0.16, 0.0087	0016570, histone modification, 21, 1, 0.02, 0.0190	0007186, G protein-coupled receptor signaling pat..., 137, 1, 0.12, 0.1190

42	5	-	-	0006368, transcription elongation from RNA polyme..., 5, 1, 0, 0.0045	0005975, carbohydrate metabolic process, 172, 2, 0.16, 0.0087	0016570, histone modification, 21, 1, 0.02, 0.0190	0007186, G protein-coupled receptor signaling pat..., 137, 1, 0.12, 0.1190
43	120	-	45	0006511, ubiquitin-dependent protein catabolic pr..., 52, 2, 0.19, 0.015	0007268, chemical synaptic transmission, 6, 1, 0.02, 0.022	0006506, GPI anchor biosynthetic process, 8, 1, 0.03, 0.029	
44	63	-	19	0008272, sulfate transport, 8, 1, 0.01, 0.011	0016055, Wnt signaling pathway, 10, 1, 0.01, 0.014		
45	556	-	198	0006468, protein phosphorylation, 215, 7, 3.23, 0.041			
46	138	-	46	0006012, galactose metabolic process, 6, 1, 0.03, 0.026	0018342, protein prenylation, 6, 1, 0.03, 0.026	0045892, negative regulation of transcription, DN..., 9, 1, 0.04, 0.038	

714

Suppl. Figure 1. Experimental design. The grey circles indicate the sampling periods.

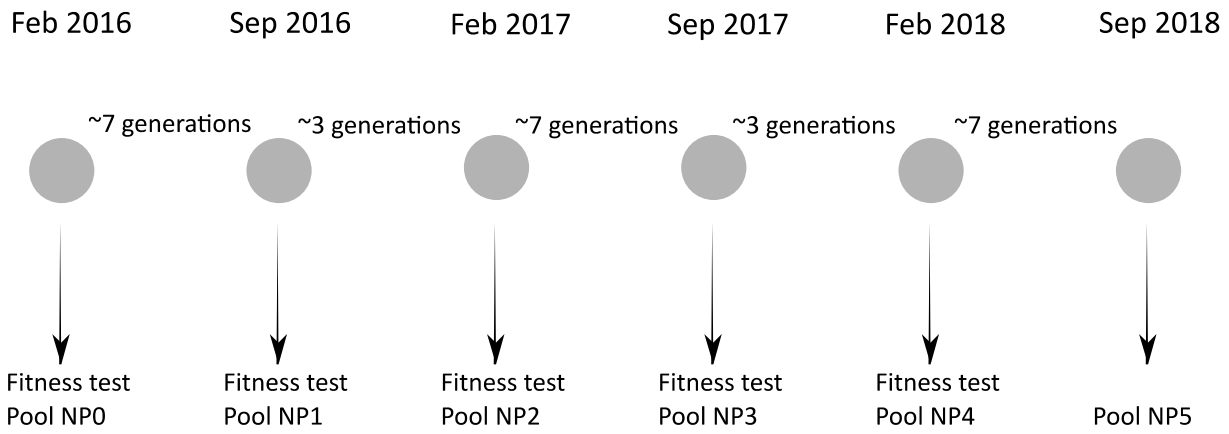

Suppl. Fig. 2. Temporal changes in mean seasonal environmental parameters in the period from 2009-2018 in the Hasselbach. The period relevant for the population genomic analyses is highlighted in grey.

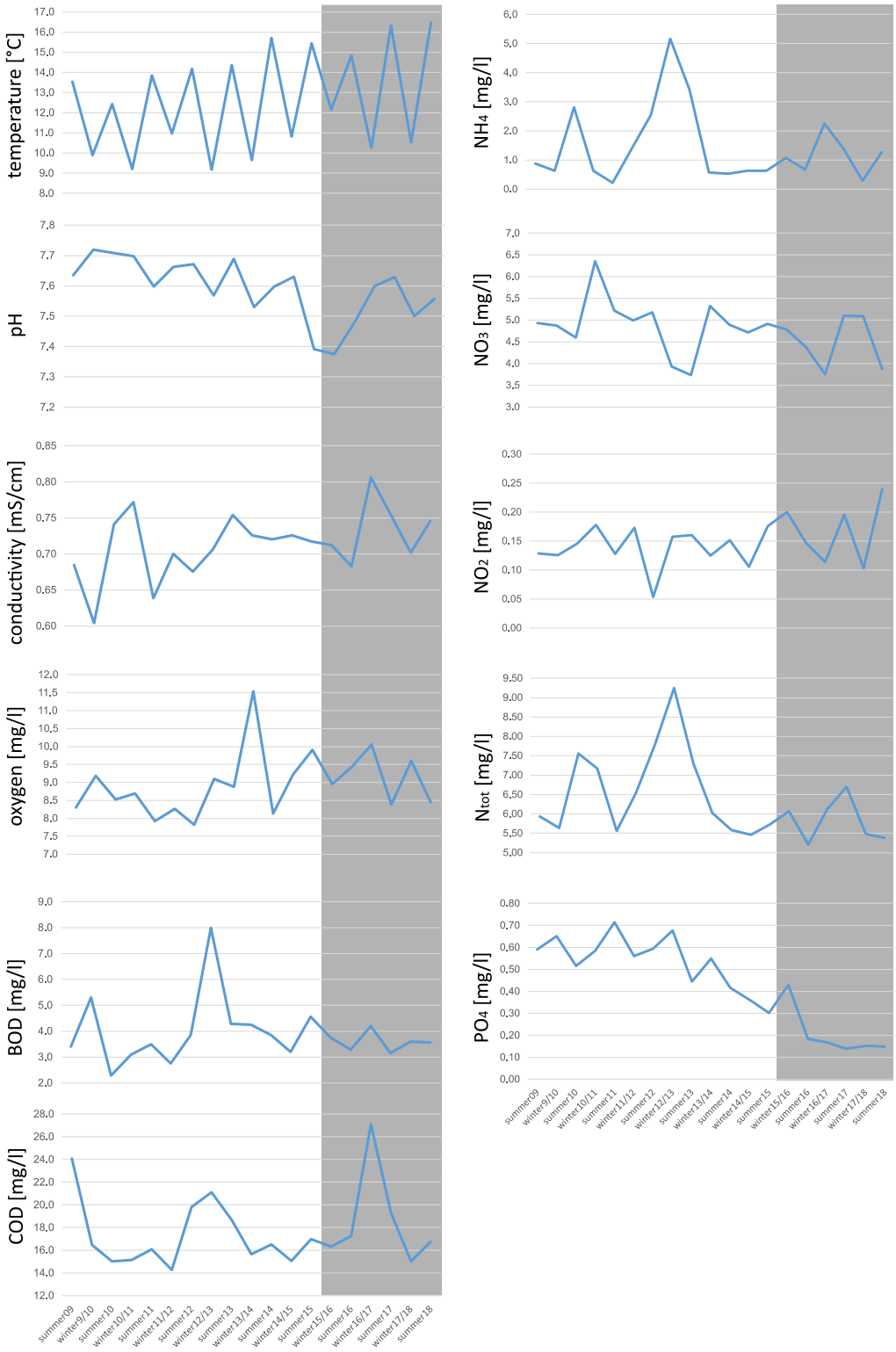

Suppl. Fig 3. Temporal autocorrelations of environmental parameters.

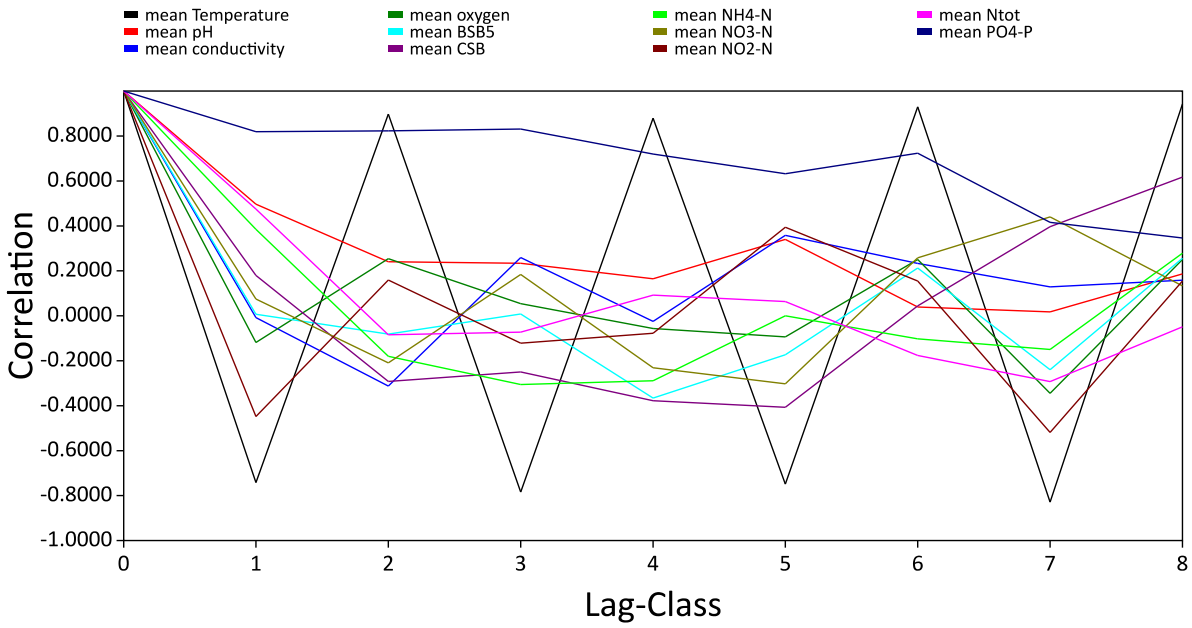

Suppl. Fig 4. Genome wide mean decay of linkage disequilibrium (r^2) in dependence of distance in basepairs.

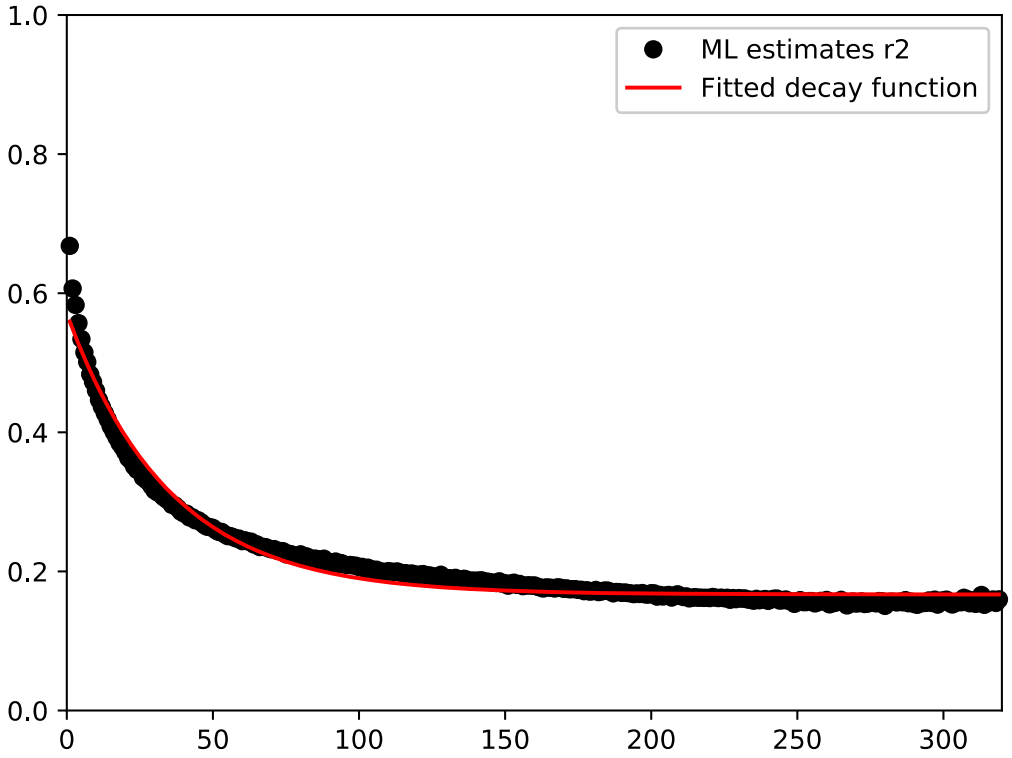

Suppl. Fig. 5. Example for inferred haplotypes of 30 re-sequenced individuals for haplotype 24 and the first SNP of haplotype 25 on scaffold 1 (positions 30800 – 31050). The marker SNPs for haplotype 24 are indicated in blue, for haplotype 25 in orange. The SNPs of haplotype 24 are in full linkage and unlinked to the SNP of haplotype 25.

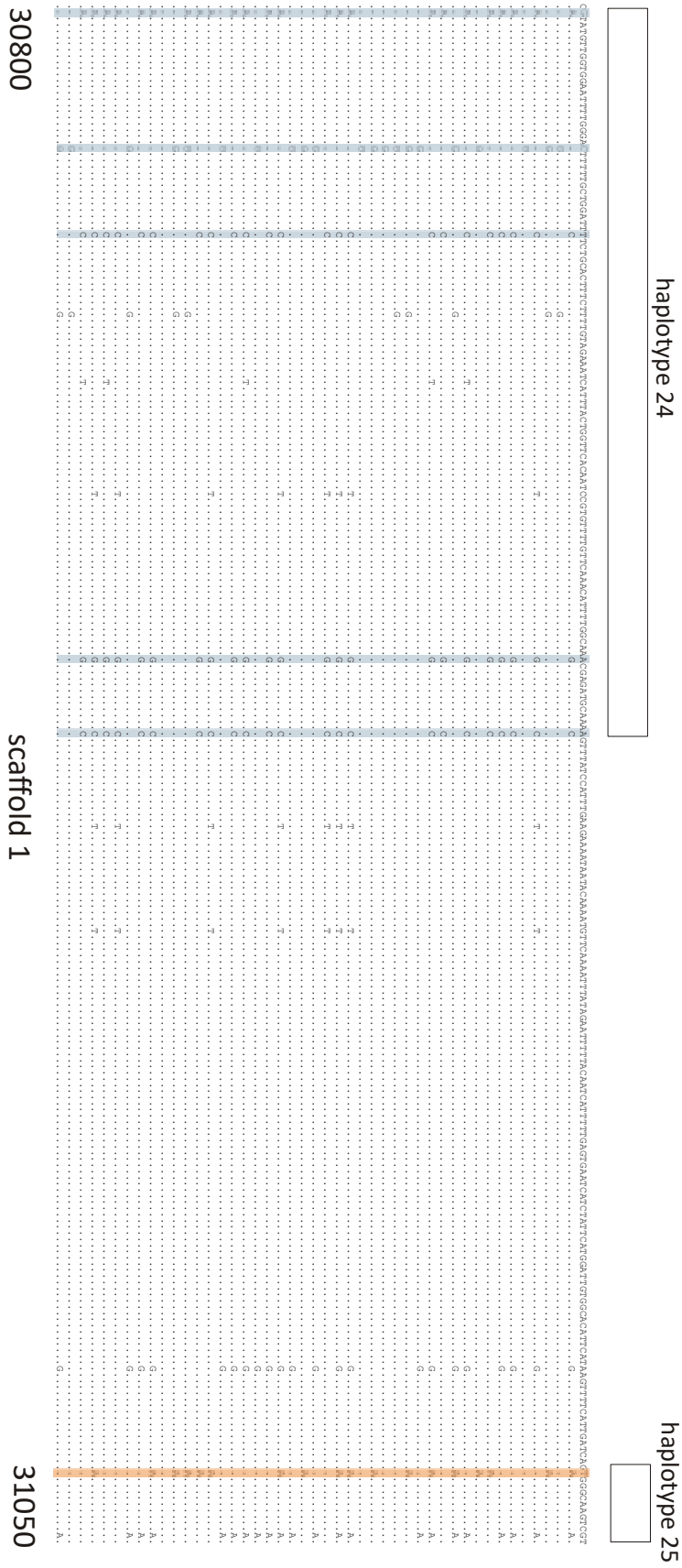
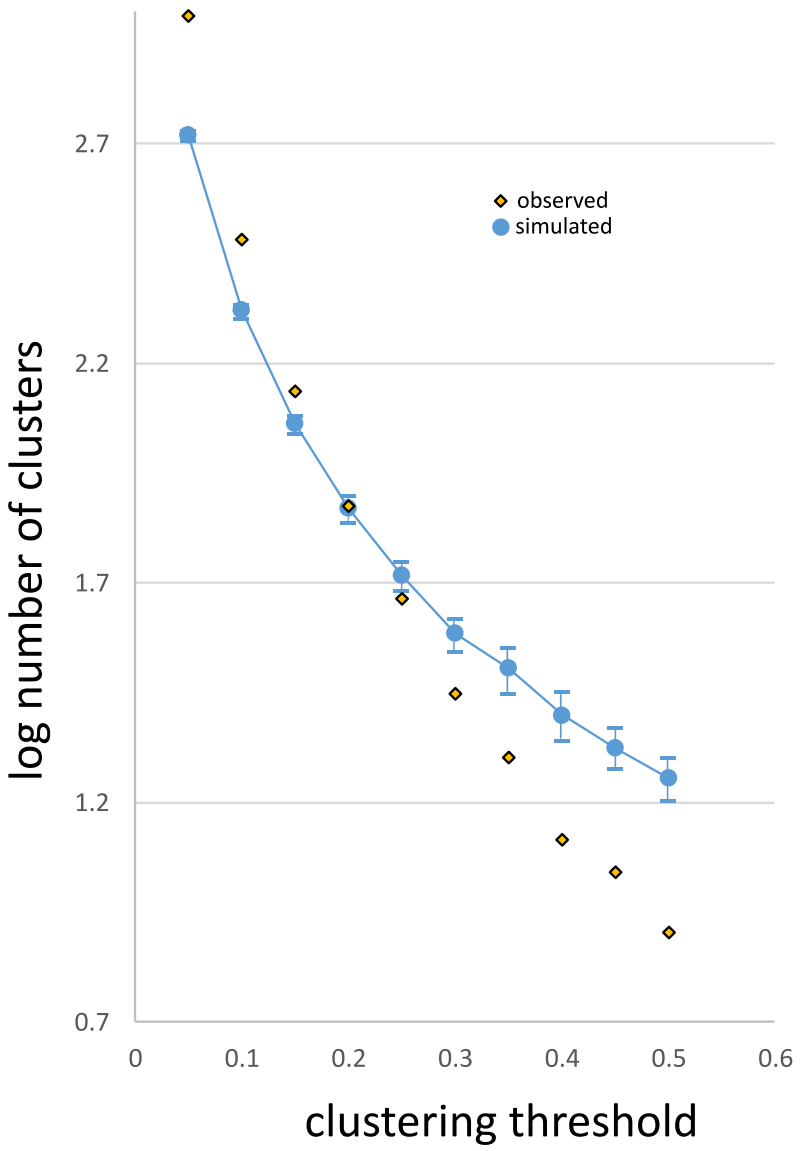
Suppl. Fig. 6. Determination of clustering threshold. Plot of clustering threshold against log number of clusters. In blue, the simulated values with 95% confidence intervals, in yellow with black outline the observed value.